

Nonlinear Aeroelastic Instability of a Supersonic Missile Wing with Pitch Axis Freeplay

Dong-Hyun Kim*

School of Mechanical and Aerospace Engineering (ReCAPT)
Gyeongsang National University (GSNU)
Gyeongsang National University, Jinju, Kyungnam, Korea 660-701

In Lee**

Department of Aerospace Engineering
Korea Advanced Institute of Science and Technology (KAIST)
373-1 Kusong-dong, Yusong-gu, Taejon, Korea 305-701

Seung-Kil Paek***

Korea Aerospace Industries (KAI), Ltd.
Sanam-myeon, Sacheon, Gyeongsangnam-do, Korea 664-942

Abstract

In this study, nonlinear aeroelastic characteristics of an supersonic missile wing with strong shock interferences are investigated. The missile wing model has a freeplay structural nonlinearity at its pitch axis. To practically consider the effects of freeplay structural nonlinearity, the fictitious mass method is applied to structural vibration analysis based on finite element method. Nonlinear aerodynamic flows with unsteady shock waves are also considered in supersonic flow regions. To solve the nonlinear aeroelastic governing equations including the freeplay effect, a modal-based coupled time-marching technique based on the fictitious mass method is used in the time-domain. Various aeroelastic computations have been performed for the nonlinear wing structure model. Linear and nonlinear aeroelastic analyses have been conducted and compared with each other in supersonic flow regions. Typical nonlinear limit cycle oscillations and phase plots are presented to show the complex vibration phenomena with simultaneous fluid-structure nonlinearities.

Key Word : Supersonic, Freeplay, Flutter, LCO, Nonlinearity, Aeroelasticity, TSD, CSD, FEM, Fluid-Structure Interaction, Fictitious Mass Method

Introduction

One of the most important problems faced by structural and design engineers is the analysis and prediction of dynamic and aeroelastic behavior (of flutter stability) of a designed wing subjected to required flight condition. An understanding of the aeroelastic behavior of flight vehicles in the transonic and supersonic regimes is of great importance for flight safety. In general, flutter calculations are performed with the assumption of a linear aerodynamic and linear structural model. However, there are two typical nonlinearities in general aeroelastic

* Assistant Professor

E-mail : dhk@gsnu.ac.kr, TEL : 055-751-6125, FAX : 055-755-2081

** Professor

*** Researcher

problems. One is aerodynamic nonlinearity and the other is structural nonlinearity. Aerodynamic nonlinearities can be attributed to shock waves, separated turbulence flow, vortex interaction, etc. Structural nonlinearities are subdivided into distributed nonlinearities and concentrated ones. Distributed nonlinearities are spread over the entire structure like material and geometric nonlinearities. However, concentrated nonlinearities have local effects in a control mechanism or an attachment of external stores etc. The concentrated structural nonlinearities typically include freeplay, friction, bilinear spring, hysteresis, and preload. Among all these several nonlinearities, the freeplay nonlinearity tends to give the most critical aeroelastic instabilities. In addition, during the service life of a flight vehicle, the level of freeplay will normally increase due to wear of bearings. Thus, most of the flight vehicles may inherently have this kind of concentrated structural nonlinearities. To date, there have been a few predominant studies on aeroelastic problems of three-dimensional wings with concentrated structural nonlinearities [1-4]. However computational studies including both the structural nonlinearity and the aerodynamic nonlinearity related to shock waves can hardly be found. The influence of the freeplay on the wing flutter characteristics can be also emphasized in the transonic and supersonic flow regions with shock waves. In addition, development of an accurate and effective computation technique is very important in the practical design process. The focus of this paper is to show the freeplay effects on nonlinear aeroelastic characteristics of an all movable wing with shock wave interferences. To effectively consider the effects of freeplay structural nonlinearity, a fictitious mass method (FMM) [5] is applied to structural vibration analysis based on finite element method (FEM). Nonlinear unsteady aerodynamics is also considered in transonic and supersonic flow regions. The TSD3KR code [6-8] based on the transonic small-disturbance equation are used to efficiently compute the transonic and supersonic aerodynamics. For the accurate time-domain solution of the nonlinear aeroelastic governing equations, a modal-based computational structural dynamic (CSD) analysis solver coupled with the fictitious mass and CFD techniques has been developed. Nonlinear aeroelastic computations for an all-movable missile wing with a pitch freeplay have been performed. Among several results, typical limit cycle oscillation (LCO) responses and phase diagrams are focused and presented in detail.

Computational Methods

Nonlinear Normal Mode Analysis

In nonlinear aeroelastic problems with concentrated structural nonlinearities, structural properties are varying as the displacement changes. Hence, using a constant normal mode from a fixed structural model gives inaccurate results. To overcome this kind of engineering problem, the fictitious mass method (FMM) [5] is applied in this study. Neglecting the effect of structural damping, free vibration (air off) equation of motion of an n degrees-of-freedom system with fictitious masses (FMs) can be given as

$$[M + M_f]\{\ddot{u}(t)\} + [K]\{u(t)\} = \{0\} \quad (1)$$

where the fictitious masses is added to the corresponding degrees-of-freedom where structural changes occur. This means that the elements of the fictitious mass matrix $[M_f]$ are zero, except for the terms added to the structure at the locations of subsequent large structural variations. From the normal mode analysis using a finite element method, the generalized mass and stiffness matrix are given as

$$[GM_f] = [\phi_f]^T [M + M_f] [\phi_f] \quad (2)$$

$$[GK_f] = [\phi_f]^T [K] [\phi_f] = [\omega_f^2] [GM_f] \quad (3)$$

where $[\phi_f]$ is a diagonal matrix of the natural frequencies including zero frequencies for rigid-body modes. Here, the size of generalized matrices directly depends on the selected number of fictitious natural vibration mode for further analysis.

It is known that the fictitious mass modes can serve as a constant set of generalized coordinates for a wide range of structural variations in the vicinity of the applied fictitious masses. Thus, it can be assumed that the displacement vector $\{u\}$ of an actual nonlinear system can be expressed as a linear combination of the fictitious mass modes as follows:

$$\{u\} = [\phi_f]\{q_f\} \tag{4}$$

Using above transformation equation, we can drive a normalized eigenvalue problem of original system as

$$[\phi_f]^T [M - M_f][\phi_f] \{\ddot{q}_f(t)\} + [\phi_f]^T [K + \Delta K][\phi_f] \{q_f(t)\} = \{0\} \tag{5}$$

or

$$([GM_f] - [\phi_f]^T [M_f][\phi_f]) \{\ddot{q}_f(t)\} + ([GK_f] - [\phi_f]^T [\Delta K][\phi_f]) \{q_f(t)\} = \{0\} \tag{6}$$

From above equations, we obtain natural frequencies, $[\omega_b] = [\omega_a]$, of the actual structure with concentrated local stiffness variations (without fictitious masses) and the base square eigenvector matrix, $[b]$. Since an all movable wing model is considered in this study, a finite element model is taking account of the stiffness variation at the pitch (or spindle) axis. Here, the accuracy of the obtained natural frequencies tends to dominantly depend on the scale of $[M_f]$. Generally, a large positive value of $[M_f]$ is strongly recommended unless inducing numerical singularity problems in calculating the eigenvalue solution of Eq. (1). By conducting some trial and error computations, we can find the appropriate large value of $[M_f]$ which gives the nicely converged solutions. The fictitious masses need to facilitate wide ranges of stiffness variations have to be significantly larger than the corresponding nominal masses of attaching nodal points.

For computational convenience, let us define the following base modal matrix as

$$[\phi_b] = [\phi_f][\bar{\chi}_b] \tag{7}$$

where $[\bar{\chi}_b]$ is a mass normalized eigenvector matrix of $[\chi_b]$ and satisfies the following relation.

$$[\bar{\chi}_b]^T ([GM_f] - [\phi_f]^T [M_f][\phi_f]) [\bar{\chi}_b] = [I] \tag{8}$$

Nonlinear Aeroelastic Analysis with Freeplay

The aeroelastic equations of motion for an elastic wing with concentrated structural nonlinearity is written as follows:

$$[M] \{\ddot{u}(t)\} + [C] \{\dot{u}(t)\} + \{R(u)\} = \{F(t, u, \dot{u})\} \tag{9}$$

where $\{R(u)\}$ is nonlinear stiffness vector which is a function of displacement. For piecewise nonlinearity, nonlinear stiffness vector can be written as follows:

$$\{R(u)\} = [KL]\{u\} + \{f(\alpha)\} \tag{10}$$

where $[KL]$ is a linear stiffness matrix of the all movable wing without pitch freeplay stiffness, and $\{f(\alpha)\}$ is the nonlinear restoring force vector whose element are zero except for nonlinear element. For a freeplay nonlinearity, $\{f(\alpha)\}$ is given as follows:

$$f(\alpha) = \begin{cases} K_a(\alpha - s), & \alpha > s \\ 0, & -s \leq \alpha \leq s \\ K_a(\alpha + s), & \alpha < -s \end{cases} \tag{11}$$

where s is a pitch displacement and α is a magnitude of freeplay angle. Let's introduce the following transformation relation based on the FMM.

$$\{u(t)\} = [\phi_b]\{q(t)\} \quad (12)$$

Using Eq. (12), the governing aeroelastic equation of motion can be reformulated in terms of generalized displacement vector $\{q(t)\}$ which is a solution of the following equation:

$$[M_g]\{\ddot{q}(t)\} + [C_g]\{\dot{q}(t)\} + \{R_g(q)\} = \{Q(t, q, \dot{q})\} \quad (13)$$

where

$$\begin{aligned} [M_g] &= [\phi_b]^T [M] [\phi_b] = [\bar{x}_b]^T ([GM_f] - [\phi_f]^T [M_f] [\phi_f]) [\bar{x}_b] \\ [C_g] &= [\phi_b]^T [C] [\phi_b] = 2[\zeta_b] [\omega_b] \\ \{R_g(q)\} &= [\phi_b]^T [KL] [\phi_b] \{q(t)\} + \{\phi_{b_r}\}^T \{f(\alpha)\} = [x_b]^T [GK_f] [x_b] \{q(t)\} + \{\phi_{b_r}\}^T \{f(\alpha)\} \\ \{Q\} &= [\bar{\phi}_b(x, y)]^T \{ \bar{F}(x, y, t) \} \\ [\bar{\phi}_b] &= [G_{kg}] [\phi_b] \end{aligned}$$

Here, $\{\phi_{b_r}\}$ is the modal displacement vector of pitch rotation and $[G_{kg}]$ is the transformation matrix for surface spline of modal matrix from FEM node to CFD grid. $\{ \bar{F}(x, y, t) \}$ is the external force vector due to unsteady aerodynamic flows around a wing. It is computed on the CFD grids of the wing surface and can be obtained by integrating the instantaneous unsteady pressure distributions as

$$\bar{F}(x, y, t) = \frac{1}{2} \rho_\infty U_\infty^2 c_r^2 \int_S (Cp_L(x, y, t) - Cp_U(x, y, t)) \frac{dS}{c_r} \quad (14)$$

In Eq. (14), unsteady pressure coefficients, C_p , are directly computed from TSD aerodynamic analyses, which are simultaneously coupled with Eq. (13). Then, the unsteady aerodynamic forces for each cell area (Eq. (14)) are numerically integrated using a two-point Gaussian quadrature formula. In this study, to fully consider the characteristics of aeroelastic responses, the coupled-time integration method (CTIM) has been used. The method is based upon the simultaneous time integration of the equations governing the coupled nonlinear fluid dynamic and structural aeroelastic system.

Introducing the state vector $\{x\}$ to perform the efficient numerical calculation, Eq. (3) can be written in the first order form as

$$\{\dot{x}(t)\} = [A]\{x(t)\} + [B]\{u(t)\} \quad (15)$$

where

$$\begin{aligned} [A] &= \begin{bmatrix} [0] & \\ -[M_g]^{-1} [x_b]^T [GK_f] [x_b] & -[M_g]^{-1} [C_g] \end{bmatrix}, \quad [B] = \begin{bmatrix} [0] \\ [M_g]^{-1} \end{bmatrix} \\ \{u(t)\} &= \begin{Bmatrix} \{0\} \\ \{Q(t)\} - [\phi]^T \{f(\alpha)\} \end{Bmatrix}, \quad \{x(t)\} = \begin{Bmatrix} q(t) \\ \dot{q}(t) \end{Bmatrix} \end{aligned}$$

Generally, to calculate the time response of Eq. (5) due to the initial condition, external forces or control inputs are needed to analyze the behavior of the system. For the nonlinear aeroelastic systems, the 5th order Runge-Kutta algorithm can be typically used for accuracy. However, for the present system with a concentrated structural nonlinearity, the stiffness can be divided by the linear wing stiffness and the nonlinear spring models. Thus, one can use more efficient and robust approach using state transition matrix. Details of numerical method can be found in Ref. 9.

Nonlinear Unsteady Aerodynamic Analysis

The flow is assumed to be that of an inviscid perfect gas. The small disturbance equation can be derived via an asymptotic expansion around flow. The modified transonic small

disturbance (TSD) potential equation transformed into the computational domain can be written in the strong conservation form as

$$\begin{aligned}
 & -\frac{\partial}{\partial \tau} \left[\frac{M^2}{\xi_x} \phi_\tau + 2M^2 \phi_\xi \right] \\
 & + \frac{\partial}{\partial \xi} \left[(1-M^2) \xi_x \phi_\xi - \frac{1}{2} (\gamma+1) M^2 \xi_x^2 \phi_\xi^2 + \frac{1}{2} (\gamma-3) M^2 (\xi_y \phi_\xi + \phi_\eta)^2 + \frac{\xi_y}{\xi_x} (\xi_y \phi_\xi + \phi_\eta) \right. \\
 & \left. - (\gamma-1) M^2 \xi_y \phi_\xi (\xi_y \phi_\xi + \phi_\eta) \right] + \frac{\partial}{\partial \eta} \left[\frac{1}{\xi_x} (\xi_y \phi_\xi + \phi_\eta) - (\gamma-1) M^2 \phi_\xi (\xi_y \phi_\xi + \phi_\eta) \right] \\
 & + \frac{\partial}{\partial \zeta} \left[\frac{1}{\xi_x} \phi_\xi \right] = 0
 \end{aligned} \tag{16}$$

where M is a freestream Mach number, ϕ is the small-disturbed potential and τ is the nondimensional time. Equation (16) is solved using a time-accurate approximate factorization (AF) algorithm. The AF algorithm consists of a time linearization procedure coupled with a Newton iteration technique. An advanced Engquist-Osher (E-O) type-dependent mixed difference operator has been also implemented in the present AF algorithm to achieve the numerical stability in the supersonic flow regions. The flow-tangency boundary condition is imposed on the wing surface. Nonreflecting far-field boundary conditions for more accurate and efficient unsteady calculations are used for both subsonic and supersonic inflow conditions. As long as separation does not occur in the flow, the TSD equations can provide a reasonable aerodynamic model for transonic and low-supersonic flutter calculations, including the modeling of aerodynamic nonlinearities that can result in limit cycle behavior. Detailed theoretical background and validation of the present study for the clean wing and the wing with control surface can be found from Ref. 6. The aerodynamic analysis results of the present approach for more advanced applications can also be found from Ref. 7.

Results and Discussion

As a computational example, the flutter of a typical all-movable wing is considered for nonlinear aeroelastic simulations with the shock wave effects. Figure 1 shows the general configuration of the present all-movable wing model. The aspect ratio of the wing is 2.564, taper ratio is 0.5, and swept-backangle of leading edge is 27.47 degree. The aerodynamic wing section is assumed as 5% biconvex airfoil. There is no aerodynamic twist but linear spanwise thickness variation. The root chord thickness and tip chord thickness are 3 mm and 1.5 mm,

Table 1. Comparison of natural frequencies for the missile wing model.

Mode	Direct Model				FM model
	$K_\alpha=120$ Nm/rad (Coupled Mass)	$K_\alpha=120$ Nm/rad (Lumped Mass)	$K_\alpha=0$ Nm/rad (Coupled Mass)	$K_\alpha=0$ Nm/rad (Lumped Mass)	$K_\alpha=120$ Nm/rad (Coupled Mass)
1	73.9 Hz	73.3 Hz	0.0 Hz	0.0 Hz	73.9 Hz
2	127.5 Hz	125.4 Hz	96.2 Hz	95.3 Hz	127.5 Hz
3	382.9 Hz	376.4 Hz	382.5 Hz	376.1 Hz	382.9 Hz
4	454.9 Hz	440.8 Hz	438.1 Hz	424.7 Hz	454.9 Hz
5	692.1 Hz	668.1 Hz	691.4 Hz	667.3 Hz	692.1 Hz
6	956.5 Hz	916.3 Hz	947.7 Hz	907.8 Hz	956.1 Hz
7	1297.3 Hz	1222.8 Hz	1296.9 Hz	1222.3 Hz	1297.4 Hz
8	1518.6 Hz	1413.8 Hz	1516.3 Hz	1410.9 Hz	1518.8 Hz

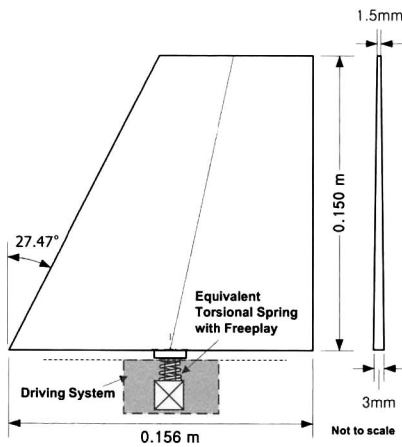


Fig. 1. Geometric configuration of the missile wing.

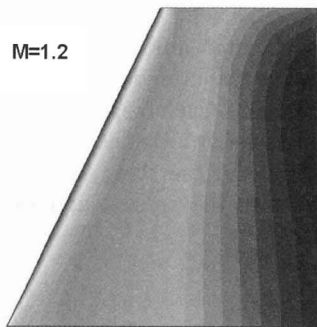


Fig. 2. Steady pressure distribution at $M=1.2$.

respectively. The material of wing is aluminum alloy and its properties are $E=72.4$ GPa, $\nu=0.33$, and $\rho=2713$ kg/m³. The finite element structural model is built up from plate, rod, spring, and concentrated mass elements. The wing is connected by a spindle axis with an equivalent torsional spring. Natural vibration analyses have been performed using MSC/NASTRAN (Ver.70.5). The plate, spring and fictitious mass are modeled as CQUAD8, CMAS2 and CELAS2 elements, respectively. The wing structure is divided by 4×4 using an eight node element (CQUAD8) with variable thickness. The effect of variable thickness is achieved using the field menu of MSC/PATRAN. Then the correct modeling of the variable thickness is verified through performing scalar plot menu of MSC/PATRAN about thickness distributions. Natural mode shape vectors are mass normalized in this study to make numerically simple computations. Considering a freeplay structural nonlinearity based on the direct finite element method usually requires a large amount of enormous computational costs so it is very inefficient. Using the fictitious mass method (FMM) can solve this kind of computational efficiency problems and give practical opportunities in using general finite element commercial code such as MSC/NASTRAN. Especially, the DMAP module can have various usability for its practical applications. In addition, MATLAB (Ver.6.0) software of the MathWorks Inc. has effectively been used in this study to conduct various matrix manipulations of the FMM procedure. It is experienced and carefully noted that double precision calculation and file printing of

data in applications of the DMAP and the MATLAB are very important to keep a high numerical accuracy. Then, those can be very useful tool for this kind of research works and to make various practical applications and rapid analysis module expansions.

For the model presented in Fig. 1, the comparison of computed lowest eight natural frequencies is summarized in Table 1. It shows that the fictitious mass model can accurately predict the natural frequencies of the original wing structure. For this computation, a concentrated mass moment of inertia (pitch rotation) of 50000 Nm² is imposed at the nodal point of a spindle connection. Because of the accuracy, the coupled mass model is used in the aeroelastic analysis. Steady pressure distribution at $M=1.2$ is presented in Fig. 2. Here one can observe the expansion shock wave on the wing surface. Surface spline technique based on the infinite plate theory is used to interpolate natural mode shapes on the aerodynamic wing surface grid. Computed first four natural mode shapes (three-dimensional view) are also presented in Fig. 3. Because of the all-movable pitch axis, low frequency mode shapes show unusual pattern in comparison with a conventional root fixed wing model. It shows that the first mode is a pitch motion dominant skewed-bending mode and the second mode is a pitch axis torsion mode. Higher modes are composed of the bending and torsion modes.

The initial angle-of-attack considered here is zero degree. The first modal displacement is applied as the initial disturbance unless otherwise stated. Figure 4 shows the free vibration responses at the wing tip leading and trailing edges. Linear and nonlinear structural model are

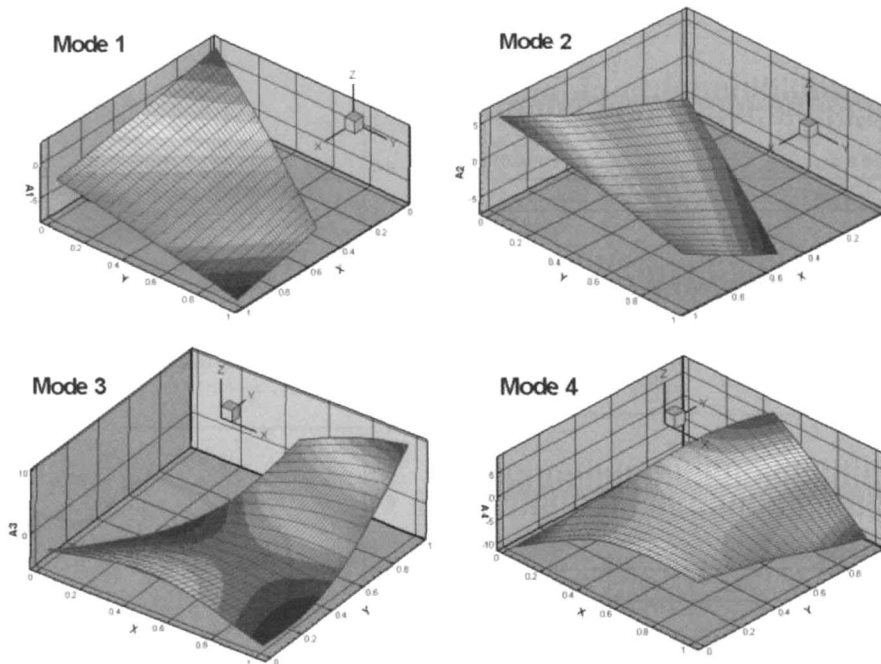


Fig. 3. Natural vibration mode shapes ($K=120 \text{ Nm/rad}$).

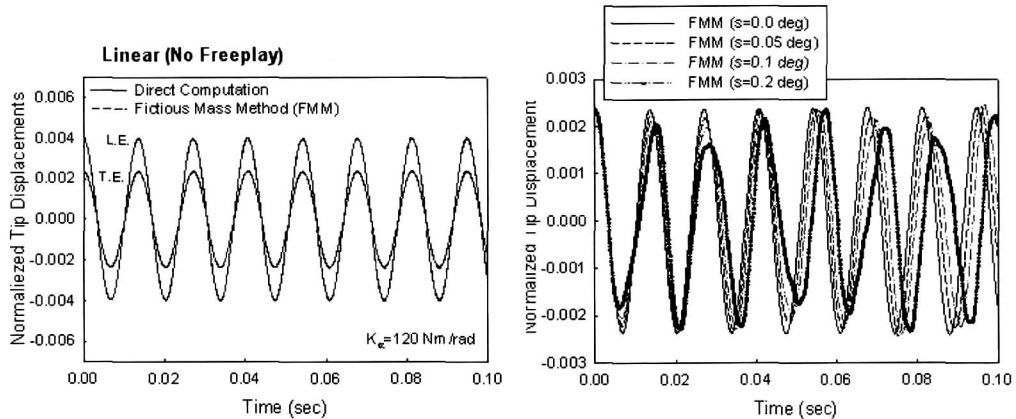


Fig. 4. Comparison of free vibration responses.

simultaneously considered to compare the basic vibration characteristic. To validate the present fictitious mass method (FMM), the FMM is compared to the direct (normal modal based) computational approach. The result of FMM shows very good agreement with that of the direct computation. Nonlinear responses for various freeplay angles are also presented to show the effect of freeplay magnitude. Here, one can see that increasing the freeplay angle, decreasing the response frequency. This physically means a reduction of equivalent torsional stiffness of the driving system. Nonlinear aeroelastic computations in the supersonic flow regime have been conducted for two-different freeplay angles: $s=0.2$ and $s=0.5$ deg. Here, dynamic pressures are normalized by the divergent flutter dynamic pressure of the case with no freeplay. This case contains two kinds of nonlinearities such as the freeplay and the transonic normal shock wave. The interaction phenomena may be especially acute and the

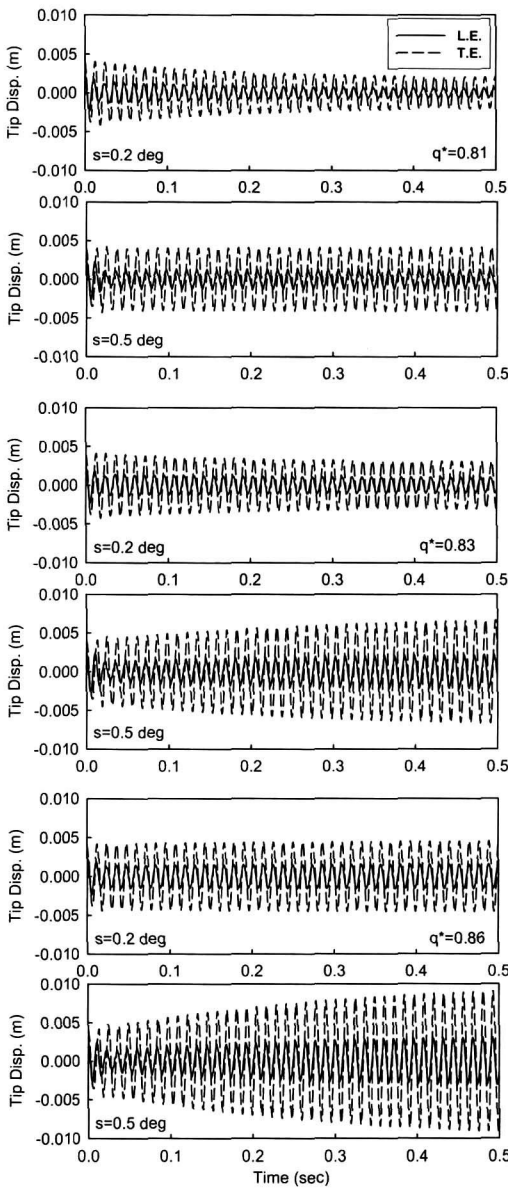


Fig. 5. Comparison of nonlinear LCO responses at wing tip ($M=1.2$).

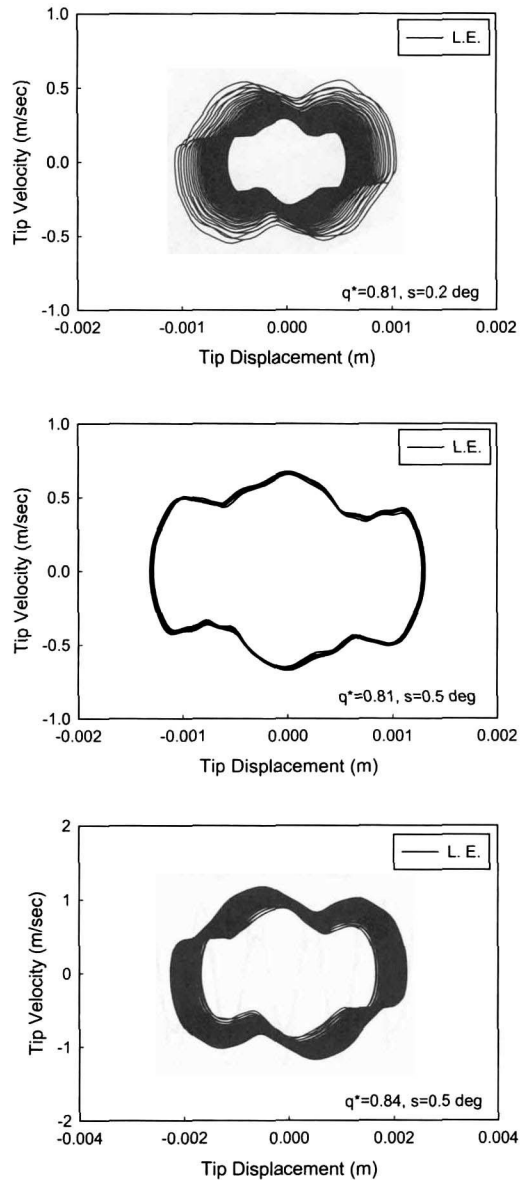


Fig. 6. Comparison of aeroelastic phase diagrams ($M=1.2$).

resultant unsteady airloads may deviate from the predictions of classical linear theory such as supersonic doublet point method (DPM). For that region, nonlinear CFD aerodynamic analysis technique is applied to increase the computational accuracy of this study. Figure 5 represents computed nonlinear responses at $M=1.2$. It shows the increment of oscillating amplitude according to an increased dynamic pressure. However, at this Mach number one can see different amplitude of oscillation at leading and trailing edges. Similar to the case of the transonic flow, the amplitude of LCO increases gradually as the freeplay angle is increased for the same dynamic pressure. Similar trend can also be found from previous studies for a two-dimensional typical section model [10]. Several phase plots for selected dynamic pressures are shown in Fig. 6. Each figure contains the nonlinear characteristic of a response. In the

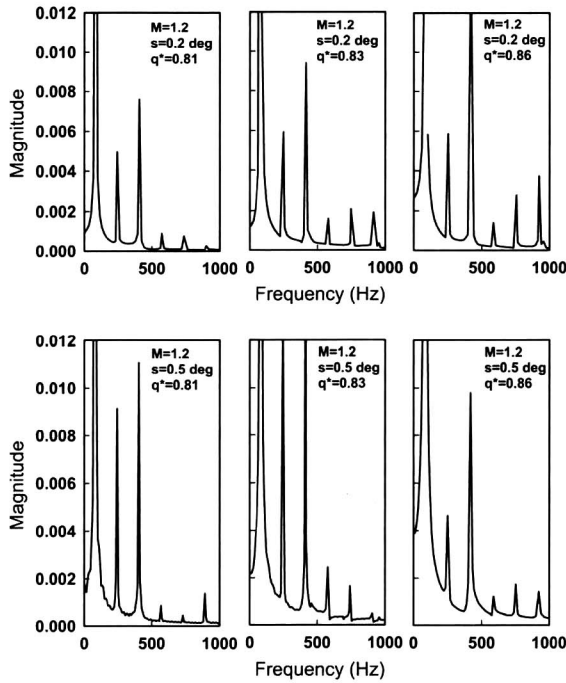


Fig. 7. Comparison of FFT results for nonlinear LCO responses.

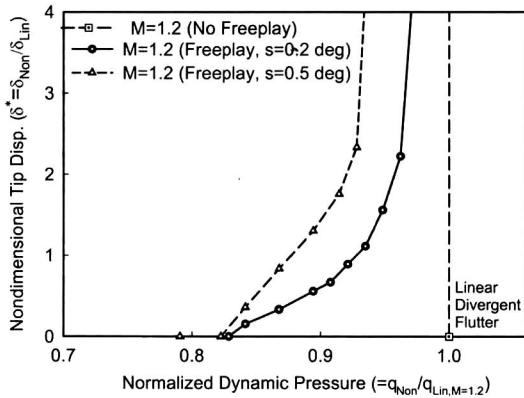


Fig. 8. Variation of LCO amplitude due to dynamic pressure change at M=1.2.

dynamic pressure. Furthermore, one can find that exponential increment of the LCO amplitude as the dynamic pressure is increased. Increasing a freeplay angle can lead to much larger LCO amplitude.

phase plots some initial disturbed responses were cut out to make more clear figures. Although not presented in this paper, responses of the leading edge tend to have much more nonlinearity than those of the trailing edge.

To clearly investigate the nonlinear aeroelastic characteristics of the aeroelastic responses, fast Fourier transform (FFT) analyses are conducted for several aeroelastic responses at the leading edge of the wing tip. Figure 7 compares selected FFT results of the wing tip responses with different freeplay angles. For the linear structural case, it tends to show only one dominant frequency for this Mach number. For the nonlinear structure cases with freeplays, one can find several multi-peaks. For these cases, as mentioned before, there are two kinds of nonlinear effects such as the structural freeplay and the aerodynamic shock wave. Magnitude of each peak indicates amount of contribution for the typical LCO phenomenon of a nonlinear aeroelastic problem. In particular, it is shown that contribution for the LCO of each natural mode can vary as the inflow Mach number, the dynamic pressure and the magnitude of a freeplay angle. To give some useful engineering insight from a design point of view, LCO amplitude diagram of the response amplitudes in the supersonic flow is presented in Fig. 8. It can be emphasized that large amplitude LCO phenomena are prone to occur at much lower dynamic pressures than divergent flutter dynamic pressures predicted by ignoring the effect of freeplay. This importantly indicates the strong possibility of detrimental structural failures or controller malfunctions before reaching a conventionally predicted flutter

Conclusions

In this study, a nonlinear aeroelastic analysis system has been developed using multidisciplinary numerical technologies. A generic all-movable missile wing with a pitch axis was considered to show the nonlinear characteristics of supersonic aeroelastic problems. One

can see the successful and practical coupling of fictitious mass method (FMM) to a typical coupled-time marching method (CTIM) using advanced CSD and CFD techniques. The results physically show that a freeplay can introduce unstable vibrations including nonlinear limit cycle oscillations in the supersonic flow region. This importantly indicates the strong possibility on detrimental structure failures or controller malfunctions at much lower flight speed than that of predicted by ignoring the effect of the freeplay. Thus, as for a safe and good performance design of an all-movable wing, it is necessary to conduct accurate analyses and investigate the complex effect of simultaneous fluid-structure nonlinearities in detail. The present computational analysis system can be a useful and cost-effective tool for the virtual flight tests on the nonlinear aeroelastic safety designs of generic high-speed flight vehicles.

Acknowledgements

This work was supported through funding from the Research Center of Aircraft Part Technology (ReCAPT) of Gyeongsang National University (GSNU) and the National Research Laboratory (NRL) program (2000-N-NL-01-C250) of Korea Ministry of Science and Technology. The authors would also like to acknowledge the supports.

References

1. Laurenson, R. M. and Trn, R. M., "Flutter Analysis of Missile Control Surfaces Containing Structural Nonlinearities," *AIAA Journal*, Vol. 18, No. 10, October 1980, pp. 1245-1251.
2. Lee, C., "An Iterative Procedure for Nonlinear Flutter Analysis," *AIAA Journal*, Vol. 24, No. 5, May 1986, pp. 833-840.
3. Lee, B. H. K. and Torn, A., "Effect of Structural Nonlinearities of the CF-18 Aircraft," *Journal of Aircraft*, Vol. 26, No. 8, August 1989, pp. 781-786.
4. Lee, I. and Kim, S. H., "Aeroelastic Analysis of a Flexible Control Surface with Structural Nonlinearity," *Journal of Aircraft*, Vol. 32, No. 4, July-August 1995, pp. 868-874.
5. Karpel, M. and Wieseman, C. D., "Modal Coordinates for Aeorelastic Analysis with Large Local Structural Variations," *Journal of Aircraft*, Vol. 31, No. 2, March-April 1994, pp. 396-400.
6. Kim, D. H., Ji, S. G., Lee, I., and Kwon, J. H., "Transonic Aerodynamic Analysis Using Transonic Small Disturbance Equation," *Journal of The Korean Society for Aeronautical and Space Sciences*, Vol. 26, No. 2, April 1998, pp. 1-9.
7. Kim, D. H. and Lee, I., "Transonic and Low-Supersonic Aerodynamic Analysis of a Wing with Underpylon/Store," *Journal of Aircraft*, Vol. 37, No. 1, January-February 2000, pp. 189-192.
8. Kim, D. H. and Lee, I., "Transonic and Supersonic Flutter Characteristics of a Wing-Box Model with Tip Stores," 42nd AIAA/ASME/ASCE/AHS/ASC Structures, Structural Dynamics, and Materials Conf. & Exhibit, Seattle, WC, 16-19 April 2001, AIAA Paper 2001-1464.
9. Kim, D. H., Park, Y. M. Lee, I. and Kwon O. J., "Nonlinear Aeroelastic Computation of a Wing with a Finned-Store Using a Parallel Unstructured Euler Solver", 43rd AIAA/ASME/ASCE/AHS/ ASC Structures, Structural Dynamics, and Materials Conf. & Exhibit, Denver, Colorado, 22-25 April 2002, AIAA Paper 1289.
10. Kim, D. H. and Lee, I., "Transonic and Low-Supersonic Aeroelastic Analysis of a Two-Degree-of-Freedom Airfoil with a Freeplay Non-Linearity," *Journal of Sound and Vibration*, Vol. 234, No. 5, 2000, pp. 859-880.